
DART: DOMAIN-ADVERSARIAL RESIDUAL-TRANSFER NETWORKS FOR UNSUPERVISED CROSS-DOMAIN IMAGE CLASSIFICATION

A PREPRINT

Xianghong Fang

SMILE Lab
Univ. of Electronic Sci & Tech.of China
Chengdu, Sichuan 611731 China

Haoli Bai

Dept Computer Science and Engineering
The Chinese University of Hong Kong
Shatin, N. T. Hong Kong, China

Ziyi Guo

SMILE Lab, Sch. of Computer Science and Engineering
University of Electronic Science and Technology of China
Chengdu, Sichuan 611731 China

Bin Shen

Google Inc.

Steven Hoi

School of Information Systems (SIS)
Singapore Management University

Zenglin Xu*

SMILE Lab, Sch. of Computer Science and Engineering
University of Electronic Science and Technology of China
Chengdu, Sichuan 611731 China
zenglin@gmail.com

January 1, 2019

ABSTRACT

The accuracy of deep learning (e.g., convolutional neural networks) for an image classification task critically relies on the amount of labeled training data. Aiming to solve an image classification task on a new domain that lacks labeled data but gains access to cheaply available unlabeled data, unsupervised domain adaptation is a promising technique to boost the performance without incurring extra labeling cost, by assuming images from different domains share some invariant characteristics. In this paper, we propose a new unsupervised domain adaptation method named Domain-Adversarial Residual-Transfer (DART) learning of Deep Neural Networks to tackle cross-domain image classification tasks. In contrast to the existing unsupervised domain adaptation approaches, the proposed DART

*Corresponding author.

not only learns domain-invariant features via adversarial training, but also achieves robust domain-adaptive classification via a residual-transfer strategy, all in an end-to-end training framework. We evaluate the performance of the proposed method for cross-domain image classification tasks on several well-known benchmark data sets, in which our method clearly outperforms the state-of-the-art approaches.

Keywords Transfer Learning · Residue Network · Adversarial Domain Adaptation

1 Introduction

Recent years have witnessed remarkable successes of deep learning methods, especially the Deep Convolutional Neural Networks (CNN), for various image classification and visual recognition tasks in multimedia and computer vision domains. The successes of deep neural networks for image classification tasks critically rely on large amounts of labeled data, usually leading to networks with millions of parameters [Lin et al., 2014, Russakovsky et al., 2015]. In practice, when solving an image categorization task in a new domain, collecting a large amount of labeled data is often difficult or very expensive, yet a large amount of unlabeled data is cheaply available. How to leverage the rich amount of unlabeled data in the target domain and to resort to an existing classification task from a source domain has become an important research topic, which is often known as unsupervised domain adaption or transfer learning [Pan and Yang, 2010, Pan et al., 2017, Wang and Deng, 2018]. The goal of this work is to explore new unsupervised domain adaption techniques for cross-domain image classification tasks.

Unsupervised domain adaptation has been actively studied in literature. One of the dominating approaches seeks to bridge source domain and target domain through learning a domain-invariant representation, and then training an adaptive classifier on the target domain by exploiting knowledge from the source domain. Following such kind of principle, several previous works have proposed to learn transferable features with deep neural networks [Long et al., 2015, Tzeng et al., 2014, Long et al., 2016, 2017, Zhuo et al., 2017], by minimizing a distance metric of domain discrepancy, such as Maximum Mean Discrepancy (MMD) [Gretton et al., 2006]. Recently, inspired by Generative Adversarial Networks (GANs) [Goodfellow et al., 2014], a surge of emerging studies proposed to apply adversarial learning for unsupervised domain adaptation [Tzeng et al., 2017, Ganin and Lempitsky, 2015, Liu and Tuzel, 2016, Liu et al., 2017, Taigman et al., 2016, Bousmalis et al., 2016, Ganin et al., 2016], validating the advantages of adversarial learning over traditional approaches in minimizing domain discrepancy and obtained new state-of-the-art results on benchmark datasets for unsupervised domain adaptation.

Among the emerging GAN-inspired approaches, DANN [Ganin et al., 2016] represents an important milestone. Based on the common low-dimensional features shared by both source and target domains, DANN introduces a domain classifier borrowing the idea from GAN to help learn transferable features. The domain classifier and the feature representation learner are trained adversarially, where the former strives to discriminate the source domain from the target domain, while the latter tries to learn domain indistinguishable features from both domains. Then a label classifier is deployed to predict the labels of samples from both domains with the learned domain-invariant features.

Despite the success of DANN, it has two major limitations. First, it assumes that the image class label classifier of the source domain can be directly applied to the target domain. However, in practice there could be some small shifts across the label classifiers in two domains, since the image classification tasks on both two domains can be quite different. An intuitive example is illustrated in the first column of Figure 1, where the source classifier fails to correctly classify data from the target domain. Second, the label information of labeled training data in the source domain is not exploited when learning the domain-invariant features. In other words, minimizing the discrepancy of marginal distributions (i.e., without exploiting label information) may only lead to some restrictive representations lacking strong class discriminative ability.

In this paper, we propose a new unsupervised domain adaptation approach named Domain-Adversarial Residual-Transfer (DART) learning for training Deep Neural Networks to tackle cross-domain image classification tasks. Specifically, the proposed DART architecture consists of three key components: image feature extractors, image label classifiers, and a domain classifier, which will be discussed in detail in Section 2. DART inherits all the advantages of DANN-based network architectures for domain-adversarial learning, but makes the following two important improvements.

First, in order to model the shifts across the label classifiers in different domains, we introduce a perturbation function across the label classifiers, and insert the ResNet [He et al., 2016] into the source label classifier to learn the perturbation function, since ResNet has demonstrated superior advantages in modelling the perturbation via a shortcut connection as shown in [Long et al., 2016]. With the learned perturbation function, the label classifier could be more robust and accurate. An intuitive illustration is shown in Figure 1, where the target classifier with the perturbation function correctly classifies image samples from the target domain.

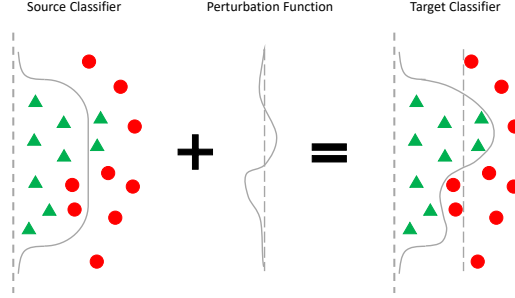


Figure 1: A well-trained source classifier may fail to classify images in the target domain correctly. By adding a perturbation function, the target classifier corrects the mistakes made by the source classifier on the target domain. Here the red dots and green triangles denote image samples from the target domain.

Second, to learn representations that are more discriminative and robust, we exploit the joint distributions of image features and class labels to align the source domain and the target domain. Specifically, our model is established based on a relaxed but more general assumption in that the joint distribution of both image data and class labels in the source domain is different from that joint distribution in the target domain. Therefore, our model seeks to reduce their joint discrepancy when learning the common feature space. Notice that class labels in the target domain are replaced by pseudo labels predicted by existing classifiers since these labels are unavailable during training in unsupervised domain adaptation. Instead of minimizing the discrepancy on marginal distributions, minimizing the joint discrepancy learns more discriminative domain-invariant features, as the joint distributions leverage the additional label information. We further regularize the model by minimizing the entropy of the predicted labels of the target domain, which ensures classification predictions from the target classifier stay away from low-density regions.

As a summary, this work makes the following major contributions:

1. Our work incorporates the learning of the perturbation function across label classifiers into the adversarial transfer network. This makes the transfer learning more adaptable to real-world image domain adaptation tasks.
2. Our work focuses on minimizing the discrepancy of the joint distributions of both image samples and class labels in the adversarial learning scheme, thus is able to yield domain-invariant features which are more discriminative .
3. We conduct extensive evaluation of cross-domain image classification on several benchmarks, in which DART clearly outperforms the state-of-the-art methods on most cases.

2 Cross-Domain Image Classification

2.1 Problem Setting

Table 1: Notations

| | |
|--------------------------------|---|
| x_i^s, x_i^t | image samples from source & target domain |
| y_i^s, y_i^t | labels from source & target domain |
| $\mathcal{D}_s, \mathcal{D}_t$ | Data of source and target domain |
| d_i^s, d_i^t | domain labels for source & target domain |
| $G_f(\cdot), G_d(\cdot)$ | feature extractor & domain classifier |
| θ | parameters for certain function |
| $\sigma(\cdot)$ | softmax function |

We consider a cross-domain image classification task by following a common setting of unsupervised domain adaption. Specifically, consider a collection of N_s image samples and class labels from a source domain $\mathcal{D}_s = \{(x_i^s, y_i^s)\}_{i=1}^{N_s}$, and N_t unlabeled image samples from a target domain $\mathcal{D}_t = \{x_i^t\}_{i=1}^{N_t}$. The goal of unsupervised cross-domain image classification is to adapt a classifier trained using only labeled data from the source domain and unlabeled data from the target domain, such that the domain-adaptive classifier can correctly predict the labels y^t of images from the target domain.

It is important to note that a major challenge of this problem is the absence of labeled data in the target domain, making it different and much more challenging from many existing supervised transfer learning problems. Another key challenge of unsupervised domain adaptation is that the source image classifier trained on the source domain \mathcal{D}_s cannot be directly applied to solve the image classification tasks in the target domain \mathcal{D}_t , because the image data between the source domain and the target domain can have large discrepancy, and their joint and marginal distributions are different, i.e. $p(x^t, y^t) \neq p(x^s, y^s)$ and $p(x^t) \neq p(x^s)$, where y^t is the true underlying target class labels.

2.2 Overview of Proposed DART

To minimize the discrepancy of the source domain and the target domain effectively, we propose the Domain-Adversarial Residual-Transfer learning (DART) of training Deep Neural Networks for unsupervised domain adaptation, as shown in Figure 2. The proposed DART method is based on two assumptions.

First of all, DART assumes the joint distributions of labels and high-level features of data should be similar. The high-level features are extracted by a feature extractor $G_f(\cdot)$ parameterized by θ_f . Then a Kronecker product is applied on high-level features and the label information to obtain joint representations. Finally, these joint representations are collectively embedded into a domain classifier $G_d(\cdot)$ parameterized by θ_d to ensure $p(G_f(x^t), \hat{y}^t) \approx p(G_f(x^s), y^s)$, where \hat{y}^t represents the predicted label.

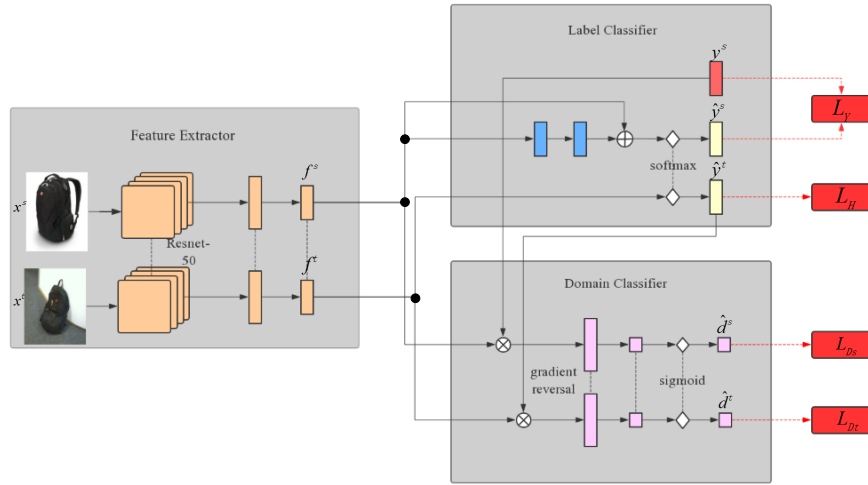


Figure 2: The architectures of Domain-Adversarial Residual-Transfer Networks (DART), which consists of a deep feature extractor (yellow), a deep label classifier (blue) and a domain classifier (purple). \oplus means the plus operator while \otimes represents the Kronecker product. The crossing lines with black points indicate connections, while crossing lines without black points are independent and not connected. The domain classifier is connected to the feature extractor via a gradient reversal layer. During the training process, we minimize the label prediction loss (source examples for \mathcal{L}_Y and target examples for \mathcal{L}_H) and the domain classification loss (for all samples). Gradient reversal ensures that the joint distributions over the two domains are made similar, thus resulting in the domain-invariant features.

Second, DART assumes the label classifier for the target domain differs from that of the source domain, and the difference between the two classifiers can be modeled by the following

$$p(y^t|x^t) = p(y^s|x^s) + \epsilon,$$

where ϵ is a perturbation function across the source label classifier $G_s(\cdot)$ and the target label classifier $G_t(\cdot)$. In order to learn the perturbation function, one way is to introduce residual layers [He et al., 2016] parameterized by θ_r by inserting into the source label classifier. Note that the predicted labels are $\hat{y}_t = G_t(G_f(x_t))$. In the following sections, we introduce each module in detail.

2.3 Domain Adversarial Training for Joint Distribution

Minimizing the domain discrepancy is crucial in learning domain-invariant features. A number of previous work seek to minimize over a metric, i.e., MMD [Gretton et al., 2006]. These methods have been proved experimentally effective, however, they suffer from large amount of hyper-parameters and thereon difficulty in training. A more elegant way is to

operate on the architecture of the neural network. DANN [Ganin et al., 2016] is a representative work in which domain discrepancy is reduced in an adversarial way, leading to an easier and faster training process.

Inspired by DANN, we devise an adversarial transfer network to collectively distinguish the joint distribution $p(G_f(x^s), y^s)$ and $p(G_f(x^t), \hat{y}^t)$. Specifically, for each domain, we fuse the high-level features from the feature extractor and labels together via a Kronecker product, i.e. $G_f(x_i^s) \otimes y_i^s$ and $G_f(x_i^t) \otimes \hat{y}_i^t$, and then embed them into the domain classifier $G_d(\cdot)$ so as to minimize the discrepancy of their joint distributions in an adversarial way. The feature extractor seeks to learn indistinguishable features from the source domain and the target domain, while the domain classifier is trained to discriminate the domain of features correctly. In the domain classifier, we manually label the source domain as $d_i^s = 1$, and the target domain as $d_i^t = 0$. We introduce the **gradient reversal layer** (GRL) as proposed in [Ganin et al., 2016] for a more feasible adversarial training scheme. Given a hyper-parameter λ and a function $f(v)$ and \cdot , the GRL can be viewed as the function $g(f(v); \lambda) = f(v)$ with its gradient $\frac{d}{dv}g(f(v); \lambda) = -\lambda \frac{d}{dv}f(v)$. With GRL, we could minimize over θ_f, θ_d directly by the standard back propagation. The output \hat{d}_i^s and \hat{d}_i^t of the domain classifier can be written as follows:

$$\begin{aligned}\hat{d}_i^s &= G_d(g(G_f(x_i^s) \otimes y_i^s)), \\ \hat{d}_i^t &= G_d(g(G_f(x_i^t) \otimes \hat{y}_i^t)).\end{aligned}\tag{1}$$

To attain precise domain prediction of joint representations, we define the loss of domain classifier as follows:

$$\begin{aligned}\mathcal{L}_D &= \mathcal{L}_{D_s} + \mathcal{L}_{D_t} \\ &= -\frac{1}{N_s} \sum_{i=1}^{N_s} d_i^s \log \hat{d}_i^s - \frac{1}{N_t} \sum_{i=1}^{N_t} (1 - d_i^t) \log (1 - \hat{d}_i^t).\end{aligned}\tag{2}$$

2.4 Residual Transfer Learning for Label Classifier Perturbation

A key point in transfer learning is to predict labels in the target domain based on the domain-invariant features. A common assumption for label classifiers is that given the domain-invariant features, the conditional distribution of labels are the equal, i.e., $p(y^t|x^t) = p(y^s|x^s)$. However, this might be insufficient to capture the underlying perturbation of label classifiers across different domains. Hence, we assume $p(y^t|x^t) = p(y^s|x^s) + \epsilon$, and consider the modelling of the perturbation between label classifiers. The residual layers [He et al., 2016] has shown its superior advantages in modelling the perturbation via a shortcut connection in RTN [Long et al., 2016], and it can be concluded by $f_s(x; \theta_r) = f_t(x) + \Delta f(x; \theta_r)$, where $\Delta f(x)$ is the perturbation function parameterized by θ_r , and $f_t(\cdot)$ is the identity function. Residual layers ensure the output to satisfy $|\Delta f(x)| \ll |f_t(x)| \approx |f_s(x)|$, as verified in [Long et al., 2016]. We set $G_s(G_f(x^s)) \triangleq \sigma(f_s(G_f(x^s)))$ and $G_t(G_f(x^t)) \triangleq \sigma(f_t(G_f(x^t))) = \sigma(G_f(x^t))$, where $\sigma(\cdot)$ is the softmax function to give specific predicted probabilities.

For the source label classifier, the loss function can be easily computed as

$$\begin{aligned}\mathcal{L}_Y &= -\frac{1}{N_s} \sum_{i=1}^{N_s} \mathcal{L}(G_s(G_f(x_i^s)), y_i^s) \\ &= -\sum_{i=1}^{N_s} \{y_i^s \log G_s(G_f(x_i^s))\}.\end{aligned}\tag{3}$$

For the target label classifier, the learned label classifier may fail in fitting the possibilities of ground truth target labels well. To tackle this problem, following [Grandvalet and Bengio, 2004], we further minimize the entropy of class-conditional distribution $p(y_i^t = j|x_i^t)$ as

$$\mathcal{L}_H = -\frac{1}{N_t} \sum_{i=1}^{N_t} \sum_{j=1}^c p(y_i^t = j|x_i^t) \log p(y_i^t = j|x_i^t).\tag{4}$$

where c represents the number of classes, and $p(y_i^t = j|x_i^t)$ can be obtained by $p(y_i^t|x_i^t) = G_t(G_f(x_i^t))$. By minimizing the entropy penalty, the target classifier G_t would adjust itself to enlarge the difference of possibilities among the predictions, and thereon predict more indicative labels.

Finally, the overall objective function of our model is

$$\mathcal{L} = \mathcal{L}_Y + \alpha \mathcal{L}_H + \beta \mathcal{L}_D.\tag{5}$$

Algorithm 1 The algorithm description for DART.

Require:

- source samples and labels (x_i^s, y_i^s) and target samples x_i^t
- domain classifier label $d_i^s = 1, d_i^t = 0$
- trade-off parameter α and β for entropy penalty and domain classification respectively and hyper-parameter $\lambda(t)$ for the gradient reversal layer function $g(\cdot; \lambda(t))$.
- the feature extractor $G_f(\cdot; \theta_f)$ with parameters θ_f ,
- the domain classifier $G_d(\cdot)$ with parameters θ_d
- the source classifier $G_s(\cdot; \theta_r)$ with parameters θ_r and target classifier $G_t(\cdot)$

for t in $[1, \text{training_steps}]$ **do****for** minibatch A, B **do**

Extract features from source samples and target samples:

$$f_i^s = G_f(x_{i \in A}^s; \theta_f, t), f_i^t = G_f(x_{i \in B}^t; \theta_f, t)$$

Obtain source label prediction and target label prediction:

$$\hat{y}_i^s = G_s(f_i^s; \theta_r, t), \hat{y}_i^t = G_t(f_i^t; t)$$

Fuse features and labels with a Kronecker product to represent joint representation:

$$z_i^s = f_i^s \otimes y_i^s, z_i^t = f_i^t \otimes \hat{y}_i^t$$

Embed joint representation into domain classifier:

$$d_i^s = G_d(g(z_i^s; \lambda(t)); \theta_d, t), d_i^t = G_d(g(z_i^t; \lambda(t)); \theta_d, t)$$

Update loss function of domain classifier:

$$\mathcal{L}_D = -\frac{1}{|A|} \sum_{i \in A} d_i^s \log \hat{d}_i^s \\ - \frac{1}{|B|} \sum_{i \in B} (1 - d_i^t) \log (1 - \hat{d}_i^t)$$

Update loss function of source classifier:

$$\mathcal{L}_Y = -\frac{1}{|A|} \sum_{i \in A} y_i^s \log \hat{y}_i^s$$

Update loss function of target classifier:

$$\mathcal{L}_H = -\frac{1}{|B|} \sum_{i \in B} \hat{y}_i^t \log \hat{y}_i^t$$

Update overall objective loss function:

$$\mathcal{L} = \mathcal{L}_Y + \alpha \mathcal{L}_H + \beta \mathcal{L}_D$$

Update θ_f, θ_d and θ_r using SGD optimizer**end for****end for****Return** $\hat{\theta}_f, \theta_d, \theta_r$

where α, β are the trade-off regularizers for the entropy penalty and the domain classification. Our goal is to find the optimal parameters $\theta_f^*, \theta_d^*, \theta_r^*$ by minimizing Equation 5.

To clearly present our DART model, we represent the pseudo-code in Algorithm 1.

3 Experiment

We evaluate the proposed DART against several state-of-the-art baselines on unsupervised domain adaptation problems. Codes and datasets will be released.

3.1 Datasets and Baselines

USPS \leftrightarrow **MNIST** : MNIST [LeCun et al., 1998] contains 60000 training digit images and 10000 test digit images, and USPS [Denker et al., 1988] contains 7291 training images and 2007 test images. For the transfer task from MNIST to USPS, we use the labeled MNIST dataset as the source domain and use unlabeled USPS dataset as the target domain, and vice versa for the transfer task from USPS to MNIST.

Office-31² [Saenko et al., 2010] is a standard benchmark for unsupervised domain adaptation. It consists of 4652 images and 31 common categories collected from three different domains: *Amazon* (**A**) which contains 2817 images from amazon.com, *DSLR* (**D**) which contains 498 images from digital SLR camera and *Webcam* (**W**) which contains 795 images from the web camera. We evaluate all methods on the following six transfer tasks: **A** \rightarrow **W**, **D** \rightarrow **W**, **W** \rightarrow **D**, **A** \rightarrow **D**, **D** \rightarrow **A**, **W** \rightarrow **A**, as done in [Long et al., 2017, 2016].

²<http://office31.com.my>

*ImageCLEF-DA*³ is a benchmark dataset for the *ImageCLEF 2014* domain adaptation challenge, consisting of three public domains: *Caltech-256*(C), *ImageNet ILSVRC 2012*(I), and *Pascal VOC 2012*(P). Each domain contains 12 categories and each category has 50 images. We also consider all the possible six transfer tasks: $I \rightarrow P$, $P \rightarrow I$, $I \rightarrow C$, $C \rightarrow I$, $C \rightarrow P$, $P \rightarrow C$, as done in [Long et al., 2017].

For MNIST to USPS and USPS to MNIST, we compare with three recent unsupervised domain adaptation algorithms: CoGAN [Liu and Tuzel, 2016], pixelDA [Bousmalis et al., 2017], and UNIT [Liu et al., 2017]. CoGAN and UNIT seek to learn the indistinguishable features from the discriminator. PixelDA is an effective method in unsupervised domain adaptation in which a generator is used to map data from the source domain to the target domain. We choose these GANs-based baselines since it has been illustrated in [Goodfellow et al., 2014] that GANs have more advantages over conventional kernel method (e.g., MMD) on reducing distribution discrepancy of domains.

For *Office-31* and *ImageCLEF-DA* datasets, in order to have a fair comparison with the latest algorithms in unsupervised domain adaptation, we choose the same baselines as reported in Joint Adaptation Network (JAN) [Long et al., 2017]. Aside from JAN, other baselines include Transfer Component Analysis (TCA) [Pan et al., 2009], Geodesic Flow Kernel (GFK) [Gong et al., 2012], ResNet [He et al., 2016], Deep Domain Confusion (DDC) [Tzeng et al., 2014], Deep Adaptation Network (DAN) [Long et al., 2015], Residual Transfer Network (RTN) [Long et al., 2016], Domain-Adversarial Training of Neural Networks (DANN) [Ganin and Lempitsky, 2015].

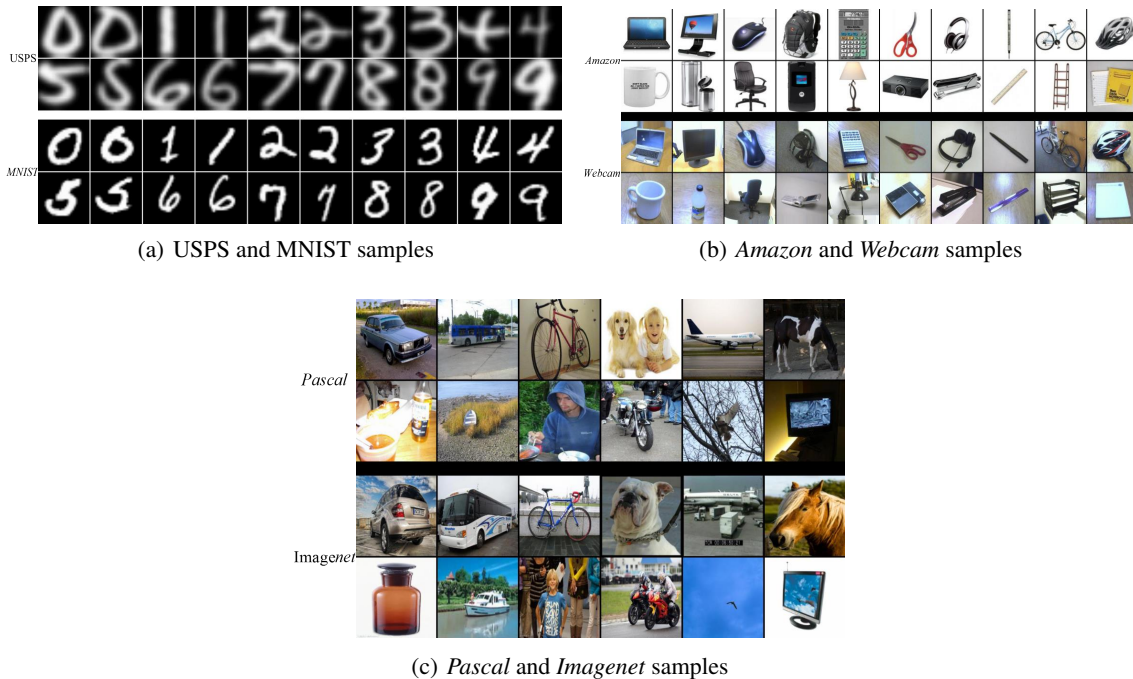
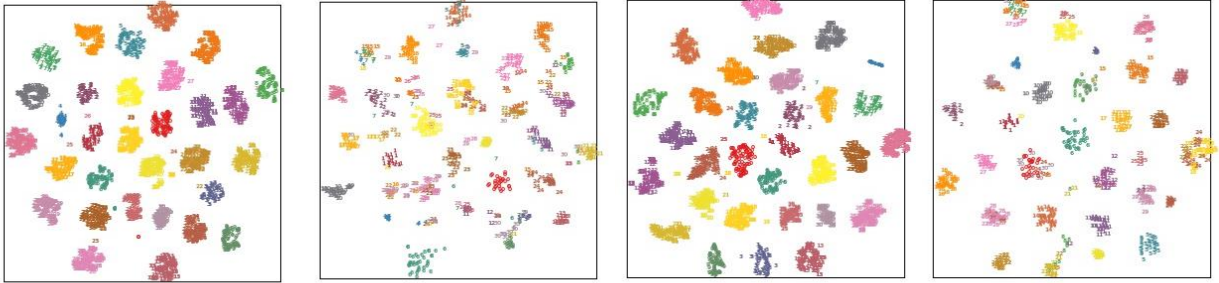


Figure 3: Experiment datasets: The first two rows in (a) (b) (c) represent examples from the USPS, Amazon and Pascal datasets, and the last two rows represent examples from the MNIST, Webcam and Imagenet datasets respectively.

3.2 Experiment Setup

Our method is implemented based on Tensorflow. We use the stochastic gradient descent (SGD) optimizer and set the learning rate $\eta = \eta_0 * \gamma^{\lfloor \frac{p}{3000} \rfloor}$, where p is the training step varying from 0 to 30000, set γ to 0.92, and set $\eta_0 \in \{0.005, 0.01, 0.02, 0.03\}$ for all transfer tasks. We fixed the trade-off regularizer weight $\alpha = 0.6$ and domain adaptation regularizer weight $\beta = 1.0$ in all experiments. In order to suppress noisy signal from the domain classifier at early stages during training, we change the hyper-parameter λ of domain classification using the following schedule: $\lambda = \lambda_0 * (\frac{2}{1 + \exp(-\gamma * q)} - 1)$, where q changes from 0 to 1 during progress, and λ_0, γ are sensitive to different datasets, as discussed in the following paragraphs.

³<http://imageclef.org/2014/adaptation>



(a) DANN: Source domain: **A** (b) DANN: Target domain: **W** (c) DART: Source domain: **A** (d) DART: Target domain **W**

Figure 4: The t-SNE visualization of network activations by DANN in (a), (b) and DART in (c), (d) respectively.

Specifically, for experiments on *Office-31* and *ImageCLEF-DA* datasets, due to the limited data in the source domain, we fine-tune our model using the pre-trained model of Resnet⁴ (50 layers) on the Imagenet [Russakovsky et al., 2015] dataset. Following the notation in ResNet, we fix the convolutional layers of conv1, conv2_x, and conv3_x, and fine-tune the rest conv4_x and conv5_x. Then we train the logits layer of ResNet, the label classifiers and the domain classifier from scratch with learning rate 10 times larger than the fine-tuning part. We set $\gamma = 10$, and $\lambda_0 \in \{1.3, 1.5, 1.8, 2.0\}$ for different tasks in *Office-31* while $\lambda_0 = 1.0$ as a fixed value for tasks in *ImageCLEF-DA*. This progressive strategy significantly stabilizes parameter sensitivity and eases model selection for DART.

For USPS and MNIST datasets, we replace the Resnet with several CNN layers without fine-tuning. We set $\lambda_0 = 1.0$, and $\gamma = 2.5$. Note that for all transfer tasks, we run our method for three times and report the average classification accuracy and the standard error for comparisons.

3.3 Results

For MNIST and USPS datasets, the classification results are shown in Table 2. The reported results of CoGAN, pixelDA, and UNIT are from their corresponding papers [Liu and Tuzel, 2016, Bousmalis et al., 2017, Liu et al., 2017]. As can be easily observed, the proposed DART outperforms all baselines on both tasks. Especially on USPS to MNIST, our model improves the accuracy by a large margin, i.e., about 6%, indicating the effectiveness of DART.

Table 2: Classification accuracy (%) on USPS and MNIST datasets.

| Model | MNIST to USPS | USPS to MNIST |
|-------------|---------------|---------------|
| CoGAN | 95.65 | 93.15 |
| pixelDA | 95.9 | - |
| UNIT | 95.97 | 93.58 |
| DART | 98.20 | 99.40 |

Similarly, the results on *Office-31* and *ImageCLEF-DA* datasets are shown in Tables 3-4. We report the results of Resnet, TCA, GFK, DDC, DAN, RTN, DANN and JAN from [Long et al., 2017], in which all the above algorithms are re-implemented. For the results of *Office-31* dataset, the proposed DART exceeds the state of the art results around 1.6% in average accuracy. In particular, on **A** \rightarrow **D**, DART achieves a large margin of improvement, i.e., more than 6.0% over the best baseline.

In terms of *ImageCLEF-DA*, the results in Table 4 again demonstrate that our model could achieve higher accuracy than the rest baselines on all transfer tasks. Compared with JAN, our average performance exceeds 1.3%.

The DART model outperforms all previous methods and sets new prediction records on most tasks, indicating its superiority of both effectiveness and robustness. DART is different from previous methods, since it adapts the joint distribution of high-level features and labels instead of marginal distributions as those in DAN, RTN and DANN, and learns the perturbation function between the label classifiers. These modifications can be the key to the improvement of the prediction performance.

⁴<https://github.com/tensorflow/models/tree/master/research/slim>

Table 3: Classification accuracy (%) on *Office-31* dataset for unsupervised domain adaptation. DART-c denotes the DART network without joint distribution alignment, and DART-s denotes the DART network without label classifier perturbation. Results of the competitive methods are copied from the original literature.

| Method | A → W | D → W | W → D | A → D | D → A | W → A | Avg |
|-------------|---------------------|---------------------|---------------------|---------------------|---------------------|---------------------|-------------|
| Resnet | 68.4 ± 0.2 | 96.7 ± 0.1 | 99.3 ± 0.1 | 68.9 ± 0.2 | 62.5 ± 0.3 | 60.7 ± 0.3 | 76.1 |
| TCA | 72.7 ± 0.0 | 96.7 ± 0.0 | 99.6 ± 0.0 | 74.1 ± 0.0 | 61.7 ± 0.0 | 60.9 ± 0.0 | 77.6 |
| GFK | 72.8 ± 0.0 | 95.0 ± 0.0 | 98.2 ± 0.0 | 74.5 ± 0.0 | 63.4 ± 0.0 | 61.0 ± 0.0 | 77.5 |
| DDC | 75.6 ± 0.2 | 96.0 ± 0.2 | 98.2 ± 0.1 | 76.5 ± 0.3 | 62.4 ± 0.4 | 61.5 ± 0.5 | 78.3 |
| DAN | 80.5 ± 0.4 | 97.1 ± 0.1 | 99.6 ± 0.1 | 78.6 ± 0.2 | 63.6 ± 0.3 | 62.8 ± 0.2 | 80.4 |
| RTN | 84.5 ± 0.2 | 96.8 ± 0.1 | 99.4 ± 0.1 | 77.5 ± 0.3 | 66.2 ± 0.2 | 64.8 ± 0.3 | 81.6 |
| DANN | 82.0 ± 0.4 | 96.9 ± 0.2 | 99.1 ± 0.1 | 79.7 ± 0.4 | 68.2 ± 0.4 | 67.4 ± 0.5 | 82.2 |
| JAN | 85.4 ± 0.3 | 97.4 ± 0.2 | 99.8 ± 0.2 | 84.7 ± 0.3 | 68.6 ± 0.3 | 70.0 ± 0.4 | 84.3 |
| JAN-A | 86.0 ± 0.4 | 96.7 ± 0.3 | 99.7 ± 0.1 | 85.1 ± 0.4 | 69.2 ± 0.2 | 70.7 ± 0.5 | 84.6 |
| DART-c | 84.5 ± 0.2 | 95.6 ± 0.1 | 98.4 ± 0.1 | 82.1 ± 0.2 | 42.4 ± 0.2 | 50.5 ± 0.3 | 75.5 |
| DART-s | 85.3 ± 0.2 | 97.6 ± 0.1 | 99.9 ± 0.1 | 86.0 ± 0.1 | 46.7 ± 0.2 | 54.3 ± 0.3 | 78.3 |
| DART | 87.3 ± 0.1 | 98.4 ± 0.1 | 99.9 ± 0.1 | 91.6 ± 0.1 | 70.3 ± 0.1 | 69.7 ± 0.1 | 86.2 |

Table 4: Classification accuracy (%) on *ImageCLEF* dataset for unsupervised domain adaptation. Results of the competitive methods are copied from the original literature.

| Method | I → P | P → I | I → C | C → I | C → P | P → C | Avg |
|-------------|---------------------|---------------------|---------------------|---------------------|---------------------|---------------------|-------------|
| Resnet | 74.8 ± 0.3 | 83.9 ± 0.1 | 91.5 ± 0.3 | 78.0 ± 0.2 | 65.5 ± 0.2 | 91.2 ± 0.3 | 80.7 |
| DAN | 74.5 ± 0.4 | 82.2 ± 0.2 | 92.8 ± 0.2 | 86.3 ± 0.4 | 69.2 ± 0.4 | 89.8 ± 0.4 | 82.5 |
| RTN | 74.6 ± 0.3 | 85.8 ± 0.1 | 94.3 ± 0.1 | 85.9 ± 0.3 | 71.7 ± 0.3 | 91.2 ± 0.4 | 83.9 |
| JAN | 76.8 ± 0.4 | 88.0 ± 0.2 | 94.7 ± 0.2 | 89.5 ± 0.3 | 74.2 ± 0.3 | 91.7 ± 0.3 | 85.8 |
| DART | 78.3 ± 0.1 | 89.3 ± 0.1 | 95.3 ± 0.1 | 91.0 ± 0.1 | 75.2 ± 0.1 | 93.5 ± 0.1 | 87.1 |

3.4 Results Analysis

Predictions Visualization: To further visualize our results, we embed the label predictions of DANN and DART using t-SNE [Donahue et al., 2014] on the example task **A** → **W**, and the results are shown in Figure 4(a)-4(d) respectively. The embeddings of DART show larger margin than those of DANN, indicating better classification performance of the target classifier of DART. Now it can be observed that the adaptation of joint distribution of features and labels is an effective approach to unsupervised domain adaptation and the modelling of the perturbation between label classifiers is a reasonable extension to previous deep feature adaptation methods.

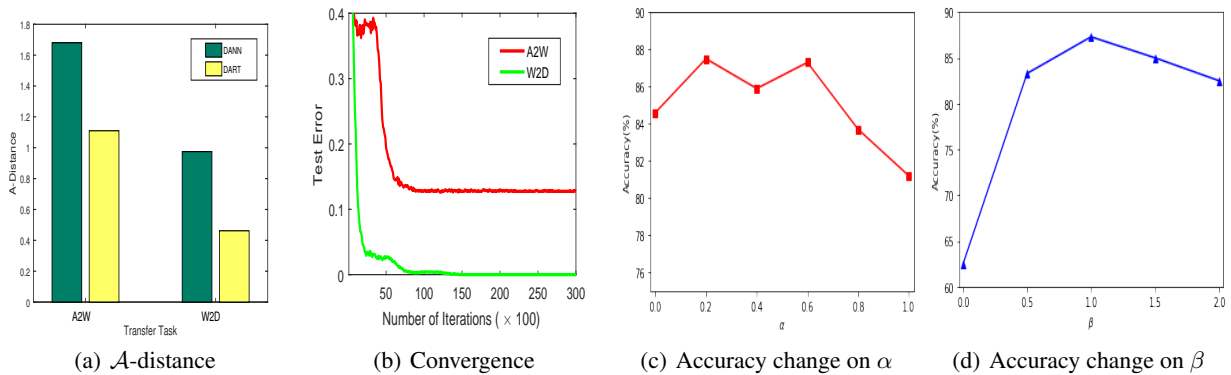


Figure 5: (a) \mathcal{A} -distance of DANN and DART; (b) The convergence performance of DART; (c) Accuracy of our model on different choice of α , with β fixed to 1.0; (d) Accuracy of the model on different choice of β , with α fixed to 0.6.

Distribution Discrepancy: We use \mathcal{A} -distance [Ben-David et al., 2009, Mansour et al., 2009] as an alternative measurement to visualize the joint discrepancy attained by DANN and DART. \mathcal{A} -distance is defined as $d_{\mathcal{A}} = 2(1 - 2\epsilon)$, where ϵ is a generalization error on some binary problems. \mathcal{A} -distance could bound the target risk when source risk is limited, i.e., $R_t(G_t) < R_s(G_s) + d_{\mathcal{A}}$, where $R_t(G_t) = E_{(x,y) \sim p(x^t, y^t)} [G_t(G_f(x)) \neq y]$ represents the target risk, and

$R_s(G_s) = E_{(x,y) \sim p(x^s, y^s)} [G_s(G_f(x)) \neq y]$ represents the source risk. Figure 5(a) shows $d_{\mathcal{A}}$ values on tasks $\mathbf{A} \rightarrow \mathbf{W}$ and $\mathbf{W} \rightarrow \mathbf{D}$ attained by DANN and DART, respectively. We observe that $d_{\mathcal{A}}$ of DART is much smaller than that of DANN, which suggests that the joint representation of features and labels in DART can bridge different domains more effectively than DANN.

Convergence Performance: To demonstrate the robustness and stability of DART, we visualize the convergence performance of our model in Figure 5(b) on two example tasks: $\mathbf{A} \rightarrow \mathbf{W}$ and $\mathbf{W} \rightarrow \mathbf{D}$. Test error of two tasks converges fast in the early 8000 steps and stabilizes in the remaining training process, which testifies the effectiveness and stability of our model.

Parameter Sensitivity Analysis: We testify the sensitivity of our model to parameters α and β , i.e. the hyper-parameters for label-classification loss and domain cross-entropy loss. As an illustration, we use task $\mathbf{A} \rightarrow \mathbf{W}$ to report the transfer accuracy of DART with different choice of α and β . Figure 5(c) reports the accuracy of varying $\alpha \in \{0.0, 0.2, 0.6, 0.8, 1.0\}$ while fixing $\beta = 1.0$. We observe that DART achieves the best performance when α is set from $[0.2, 0.6]$, although there is a vibration when $\alpha = 0.4$. The vibration may be caused by the small number of samples. As for β , the best accuracy can be obtained when setting β from $[0.5, 1.5]$, illustrating a bell-shaped curve as showed in Figure 5(d).

Table 5: Categories of Unsupervised Domain Adaptation Methods

| Model | Discrepancy measure | Distribution assumption | Classifier Perturbation |
|----------------------------------|-----------------------------|-------------------------|-------------------------|
| DDC [Tzeng et al., 2014] | MMD | Marginal | no |
| DAN [Long et al., 2015] | MMD | Marginal | no |
| DANN [Ganin et al., 2016] | Domain Adversarial Loss | Marginal | no |
| DSN [Bousmalis et al., 2016] | MMD/Domain Adversarial Loss | Marginal | no |
| UNIT [Liu et al., 2017] | GAN | Marginal | no |
| CoGAN [Liu and Tuzel, 2016] | GAN | Marginal | no |
| DTN [Taigman et al., 2016] | GAN | Marginal | no |
| pixelDA [Bousmalis et al., 2017] | GAN | Marginal | no |
| RTN [Long et al., 2016] | MMD | Marginal | yes |
| JDA [Long et al., 2013] | MMD | Joint | no |
| JAN [Long et al., 2017] | JMMD | Joint | no |
| DART(proposed) | Domain Adversarial Loss | Joint | yes |

4 Related work

Unsupervised domain adaptation based on deep learning architectures can bridge different domains or tasks and mitigate the burden of manual labeling. The goal of domain adaptation is to reduce the domain discrepancy measured in various probability distributions of different domains. In the following, we review different deep domain adaptations methods from three perspectives: (1) domain discrepancy measures; (2) distributions used to measure the discrepancy; (3) differences between label classifiers of both domains.

In unsupervised domain adaptation, most methods try to learn domain-invariant features, such as DDC [Tzeng et al., 2014], DAN [Long et al., 2015], DANN [Ganin et al., 2016], Conditional Adversarial Domain Adaptation [Long et al., 2018], etc. That means $p(G_s(x^t)) \approx p(G_t(x^s))$. Recent approaches assume that both the source domain and the target domain should share a joint distribution of both features and labels. That means the joint distributions of extracted features and labels are shared, i.e., $p(G_s(x^t), y^t) \approx p(G_t(x^s), y^s)$. Such work include JDA [Long et al., 2013] and JAN [Long et al., 2017]. Our work follows the idea of JDA to model the joint distribution, and use the Kronecker project to generate feature and label maps.

In terms of measuring the distribution alignment between the source domain and the target domain, most of previous methods have utilized probabilistic measures, such as the Maximum Mean Discrepancy (MMD) and [Gretton et al., 2006], the correlation alignment [Sun and Saenko, 2016]. DDC [Tzeng et al., 2014] and DAN [Long et al., 2015] minimizes the discrepancy such that a representation that is both semantically meaningful and domain-invariant can be learned. Recent methods have utilized the idea of adversarial learning to implicitly measure the distribution alignment between the source domain and the target domain. Among these methods, UNIT [Liu et al., 2017] and CoGAN [Liu and Tuzel, 2016] adopt GANs in their architectures to generate domain translated images and evaluate whether the translated images are realistic for each domain; while DTN [Taigman et al., 2016] and pixelDA [Bousmalis et al., 2017] map data in the source domain to the target domain by a generator. DANN [Ganin et al., 2016] introduces a domain

classifier borrowing the idea from adversarial training to help learn transferable features. The proposed DART follows the idea of DANN to discriminate features from the source domain and the target domain.

In terms of the relation between the source classifier and the target classifier, previous unsupervised domain adaptation methods mostly assume that the same conditional distribution is shared between the target domain and the source domain, i.e., $p(y^t|x^t) = p(y^s|x^s)$. Different from this category of approaches, the second category relaxes the rather strong assumption. Instead, it considers a more general scenario in practical applications and assumes that the source classifier and the target classifier differ by a small perturbation function. RTN [Long et al., 2016] learns an adaptive classifier by adding residual modules into the source label classifier, fusing the features from multiple layers with a Kronecker product, and then minimizing its discrepancy.

Taking the advantages of successful unsupervised domain adaptation methods, we design our DART by introducing perturbation to the source classifier and the target classifier to increase flexibility, measuring the joint distributions of features and labels, and introducing the domain adversarial loss to discriminate two domains.

5 Conclusion

This paper presents a novel approach to the unsupervised domain adaptation in deep networks, which enables the end-to-end learning of adaptive classifiers and transferable features. Unlike previous methods that match the marginal distributions of features across different domains, the proposed approach reduces the discrepancy of domains using the joint distribution of both high-level features and labels. In addition, the proposed approach also learns the perturbation function across the label classifiers via the residual modules, bridging the source classifier and target classifier together to produce more robust outputs. The approach can be trained by standard back-propagation, which is scalable and can be implemented by most deep learning packages. We conduct extensive experiments on several benchmark datasets, validating the effectiveness and robustness of our model. Future work constitutes semi-supervised domain adaptation extensions.

References

- Shai Ben-David, John Blitzer, Koby Crammer, Alex Kulesza, Fernando Pereira, and Jennifer Wortman Vaughan. A theory of learning from different domains. *Machine Learning*, 79:151–175, 2009.
- Konstantinos Bousmalis, George Trigeorgis, Nathan Silberman, Dilip Krishnan, and Dumitru Erhan. Domain separation networks. In *NIPS*, 2016.
- Konstantinos Bousmalis, Nathan Silberman, David Dohan, Dumitru Erhan, and Dilip Krishnan. Unsupervised pixel-level domain adaptation with generative adversarial networks. In *2017 IEEE Conference on Computer Vision and Pattern Recognition, CVPR 2017, Honolulu, HI, USA, July 21-26, 2017*, pages 95–104, 2017.
- John S. Denker, W. R. Gardner, Hans Peter Graf, Donnie Henderson, Richard E. Howard, Wayne E. Hubbard, Lawrence D. Jackel, Henry S. Baird, and Isabelle Guyon. Neural network recognizer for hand-written zip code digits. In *NIPS*, 1988.
- Jeff Donahue, Yangqing Jia, Oriol Vinyals, Judy Hoffman, Ning Zhang, Eric Tzeng, and Trevor Darrell. Decaf: A deep convolutional activation feature for generic visual recognition. In *ICML*, 2014.
- Yaroslav Ganin and Victor S. Lempitsky. Unsupervised domain adaptation by backpropagation. In *ICML*, 2015.
- Yaroslav Ganin, Evgeniya Ustinova, Hana Ajakan, Pascal Germain, Hugo Larochelle, François Laviolette, Mario Marchand, and Victor Lempitsky. Domain-adversarial training of neural networks. *Journal of Machine Learning Research*, 17(59):1–35, 2016.
- Boqing Gong, Yuan Shi, Fei Sha, and Kristen Grauman. Geodesic flow kernel for unsupervised domain adaptation. *2012 IEEE Conference on Computer Vision and Pattern Recognition*, pages 2066–2073, 2012.
- Ian J. Goodfellow, Jean Pouget-Abadie, Mehdi Mirza, Bing Xu, David Warde-Farley, Sherjil Ozair, Aaron C. Courville, and Yoshua Bengio. Generative adversarial nets. In *NIPS*, 2014.
- Yves Grandvalet and Yoshua Bengio. Semi-supervised learning by entropy minimization. In *NIPS*, 2004.
- Arthur Gretton, Karsten M. Borgwardt, Malte J. Rasch, and Bernhard. A kernel method for the two-sample-problem. In *NIPS*, 2006.

- Kaiming He, Xiangyu Zhang, Shaoqing Ren, and Jian Sun. Deep residual learning for image recognition. *2016 IEEE Conference on Computer Vision and Pattern Recognition (CVPR)*, pages 770–778, 2016.
- Yann LeCun, Léon Bottou, Yoshua Bengio, and Patrick Haffner. Gradient-based learning applied to document recognition. *Proceedings of the IEEE*, 86(11):2278–2324, 1998.
- Tsung-Yi Lin, Michael Maire, Serge J. Belongie, James Hays, Pietro Perona, Deva Ramanan, Piotr Dollár, and C. Lawrence Zitnick. Microsoft coco: Common objects in context. In *ECCV*, 2014.
- Ming-Yu Liu and Oncel Tuzel. Coupled generative adversarial networks. In *NIPS*, 2016.
- Ming-Yu Liu, Thomas Breuel, and Jan Kautz. Unsupervised image-to-image translation networks. *CoRR*, abs/1703.00848, 2017.
- Mingsheng Long, Jianmin Wang, Guiguang Ding, Jia-Guang Sun, and Philip S. Yu. Transfer feature learning with joint distribution adaptation. *2013 IEEE International Conference on Computer Vision*, pages 2200–2207, 2013.
- Mingsheng Long, Yue Cao, Jianmin Wang, and Michael I. Jordan. Learning transferable features with deep adaptation networks. In *ICML*, 2015.
- Mingsheng Long, Han Zhu, Jianmin Wang, and Michael I. Jordan. Unsupervised domain adaptation with residual transfer networks. In *NIPS*, 2016.
- Mingsheng Long, Jianmin Wang, and Michael I. Jordan. Deep transfer learning with joint adaptation networks. In *ICML*, 2017.
- Mingsheng Long, ZHANGJIE CAO, Jianmin Wang, and Michael I Jordan. Conditional adversarial domain adaptation. In S. Bengio, H. Wallach, H. Larochelle, K. Grauman, N. Cesa-Bianchi, and R. Garnett, editors, *Advances in Neural Information Processing Systems 31*, pages 1647–1657. 2018.
- Yishay Mansour, Mehryar Mohri, and Afshin Rostamizadeh. Domain adaptation: Learning bounds and algorithms. In *In Proceedings of COLT*. Citeseer, 2009.
- Sinno Jialin Pan and Qiang Yang. A survey on transfer learning. *IEEE Transactions on Knowledge and Data Engineering*, 22:1345–1359, 2010.
- Sinno Jialin Pan, Ivor W. Tsang, James T. Kwok, and Qiang Yang. Domain adaptation via transfer component analysis. *IEEE Transactions on Neural Networks*, 22:199–210, 2009.
- Yingwei Pan, Ting Yao, Houqiang Li, and Tao Mei. Video captioning with transferred semantic attributes. In *2017 IEEE Conference on Computer Vision and Pattern Recognition, CVPR 2017, Honolulu, HI, USA, July 21-26, 2017*, pages 984–992, 2017.
- Olga Russakovsky, Jia Deng, Hao Su, Jonathan Krause, Sanjeev Satheesh, Sean Ma, Zhiheng Huang, Andrej Karpathy, Aditya Khosla, Michael S. Bernstein, Alexander C. Berg, and Li Fei-Fei. Imagenet large scale visual recognition challenge. *International Journal of Computer Vision*, 115:211–252, 2015.
- Kate Saenko, Brian Kulis, Mario Fritz, and Trevor Darrell. Adapting visual category models to new domains. In *ECCV*, 2010.
- Baochen Sun and Kate Saenko. Deep coral: Correlation alignment for deep domain adaptation. In *ECCV Workshops*, 2016.
- Yaniv Taigman, Adam Polyak, and Lior Wolf. Unsupervised cross-domain image generation. *CoRR*, abs/1611.02200, 2016.
- Eric Tzeng, Judy Hoffman, Ning Zhang, Kate Saenko, and Trevor Darrell. Deep domain confusion: Maximizing for domain invariance. *CoRR*, abs/1412.3474, 2014.
- Eric Tzeng, Judy Hoffman, Kate Saenko, and Trevor Darrell. Adversarial discriminative domain adaptation. *CoRR*, abs/1702.05464, 2017.
- Mei Wang and Weihong Deng. Deep visual domain adaptation: A survey. *Neurocomputing*, 312:135–153, 2018.
- Junbao Zhuo, Shuhui Wang, Weigang Zhang, and Qingming Huang. Deep unsupervised convolutional domain adaptation. In *Proceedings of the 2017 ACM on Multimedia Conference, MM '17*, pages 261–269, 2017. ISBN 978-1-4503-4906-2.